

Epsilon Aurigae

I. Multi-ring structure of the eclipsing body

S. Ferluga

Dipartimento di Astronomia, Università di Trieste, via G.B. Tiepolo, 11, I-34131 Trieste, Italy

Received December 5, 1989; accepted April 7, 1990

Abstract. The geometry of the eclipsing component of ϵ Aur is investigated here by using the method of the synthetic light curve. Evidence is found that the eclipsing body is a *system of rings*, encircling the secondary, and forming a thin disk with a central aperture. The structure is seen almost edge-on, and globally it appears as a composite ring, flat and extended, consisting of concentric bands with different transparencies.

On the last eclipse during 1983, the following features were recognized: a large central aperture ($r = 1.6$ AU), a semitransparent outer edge of the disk ($r = 5.9$ AU), and a transparent annular zone ($r = 3.1$ AU; width = 0.8 AU) splitting the main opaque ring into two concentric bands. The inclination of the disk plane with respect to the sky is found to be $j = 82^\circ$ (while the inclination of the orbit, $i = 89.4^\circ$, and the tilt of the disk, $\psi = 2.3^\circ$ are given by photopolarimetry).

Secular variability of the ring system is analysed, by applying the same method to previous eclipses (1929 and 1956). Only minor features appear to be variable, e.g. the relative extension of concentric bands, and the sharpness of the external edge of the disk.

The rings may consist of dust, formed by accretion of particles (primary's wind) onto stable orbits around the secondary, which is probably a close binary (triple-system model).

Key words: accretion disks – stars: binaries: spectroscopic – stars: binaries: general – stars: circumstellar matter – stars: ϵ Aur – stars: variable.

1. Introduction

The system of ϵ Aur comprises a primary star (apparently a normal F0 supergiant), with a peculiar companion which is obscure at visible wavelengths. The period of the system is 27.1 years, and only the primary eclipse can be seen. The eclipse lasts about 2 years, and at visible wavelengths it is ~ 0.75 mag deep and almost grey.

The most recent eclipse was observed in 1982–84, and it has been investigated extensively (Stencel, 1985; Swings, 1986); two earlier events in 1929 and 1956 are also well documented. The eclipsing companion – although obscure in the visible – does

Send offprint requests to: S. Ferluga.

emit both in the UV with a $T_{\text{eff}} \simeq 13000$ K, and in the IR with a $T_{\text{eff}} \simeq 750$ K. This fact, which is proved by the reduced eclipse depth in the UV and IR, indicates the presence of a hot stellar source, embedded in a large cool eclipsing body.

The masses of the components are difficult to determine (only the mass function is known). The *large-mass* model ($q \simeq 1$) considers the primary to be a normal F supergiant of about $15 M_\odot$ (Wright, 1970); while the *small-mass* model ($q \simeq 1/4$) assumes that the primary is an undermassive evolved star of about $1 M_\odot$ (Eggleton and Pringle, 1985). Moreover, the secondary itself is probably a close binary, with early-m.s. components (Lissauer and Backman, 1984), and this would explain its low luminosity, with respect to the large mass implied by the $q \simeq 1$ model.

The shape of the eclipsing body can be deduced from the light-curve features. Since the minimum is almost flat (like in a total eclipse) but the primary spectrum remains visible (like in a partial eclipse), the phenomenon is interpreted as due to the partial occultation of the F-star's surface by an elongated opaque object. Geometrical models of the eclipsing body, in terms of an inclined disk, were developed by Wilson (1971), Huang (1974), and others.

The purpose of this paper is to investigate the structure of the eclipsing object, by performing a fine analysis of the light curve with the aid of numerical simulation techniques.

2. The mid-eclipse brightening in 1983

The most complete photometric coverage for the latest eclipse of 1982–84 is reported by Schmidtke (1985), combining *UBV* light curves from different observatories. A striking feature, appearing in both the *V* and *B* light curves (*U* data being poor), is a remarkable brightening of about 0.2 mag (Fig. 1, dots), centered at mid totality and lasting for about 7 months (Mar–Sep'83). Regrettably, the observational coverage of the light curve is interrupted just near mid eclipse (owing to seasonal proximity of the sun), so that the peak of the brightening is not recorded. However, the available data are sufficient for deriving basic indications about the origin of the phenomenon, as well as univocal conclusions about the geometry of the object responsible for the observed eclipse.

First of all, there is evidence that the brightening at mid totality is really due to the eclipsing body, and is not related with intrinsic variability (commonly occurring out of eclipse,

and observed also at 3rd contact by Ôki *et al.*, 1984). The correlation with the eclipse is clear, since the brightening is almost colorless, like all the other eclipse-dependent variations (while intrinsic activity is enhanced at short wavelengths), and moreover the brightening acts only upon the spectral continuum without affecting the lines (as noted in the ultraviolet by Ferluga and Hack, 1985). This behaviour leads straight to the following interpretation: during the latest eclipse, a remarkable central *rarefaction* has been observed in the middle of the almost-grey eclipsing body.

This casts new light on the geometrical models of the eclipsing object, resuming the long-standing alternative between: (i) a thick semitransparent disk seen edge-on with a central cavity (Huang, 1974), and (ii) a thin opaque disk seen obliquely with a central aperture (Wilson, 1971). Both configurations, assuming a planar disk about 5 times larger than the eclipsed supergiant (that is, with a diameter of ~ 10 AU), in principle can explain the observed attenuation of 50% in luminosity (0.75 mag) during totality, as well as the permanence of the primary spectrum during the whole eclipse.

In fact, the *thick disk* (i) is supposed to be at least as thick as the primary's diameter, and it should be 50%-transmittant when viewed edge-on; so it would appear like an elongated semi-transparent screen, veiling the entire surface of the eclipsed star. On the other side, the *thin disk* (ii) is supposed to be generally opaque; thus, when viewed at grazing incidence (few degrees), it would appear like an elongated obscure band, occulting about 50% of the surface of the eclipsed star.

Now, the properties of the present brightening, namely its considerable height $\Delta m \simeq 0.2$ mag and its comparably short duration $\Delta t \simeq 200$ d, are significant enough to lead us to abandon the thick-disk hypothesis (i). Although this fact was already quoted by other authors (e.g. Van Hamme and Wilson, 1986), let us examine the argument in more detail.

3. Thick disk or thin disk ?

The overall duration of the brightening in 1983 is about twice a partial-eclipse phase (ingress or egress). If the phenomenon is generated by a cavity inside a *thick disk*, then the size of the cavity should be about the same as the size of the eclipsed star, that is $\sim 1/5$ of the disk size. In this case, for producing the most prominent brightening at mid eclipse, there would have to be a totally transparent cavity, in the center of the semitransparent disk.

The mid-eclipse brightening is produced when the central cavity transits in front of the eclipsed star. As the radius of the cavity is only $\sim 1/5$ of the disk radius, the corresponding reduction in optical depth will produce a mid-eclipse brightening hardly reaching 0.1 mag; but this is only one half of the observed amplitude. Equivalently, in order to match the observed 0.2 mag amplitude, one could consider a cavity almost double in size; but this would imply a corresponding duration of the brightening almost twice as long as that observed. In conclusion, the thick-disk geometry produces a mid-eclipse brightening which is by far too smooth, with respect to the observed one.

On the contrary, a *thin-disk* configuration, with a central aperture of about the same size as the eclipsed star ($\sim 1/5$ of the disk size), or a little larger, can in principle produce a mid-eclipse brightening which is high and sharp enough. In fact such an eclipsing body, seen at grazing incidence ($\sim 5^\circ$), when transiting

in front of the star's equator, will be able to occult about 50% of the stellar surface, thus producing the observed eclipse depth of 0.75 mag. Moreover, let us consider a central hole of 1.2 stellar radii (still compatible with the eclipse duration): at mid eclipse, through this aperture an additional 10% of the stellar surface will be seen, thus producing the observed 0.2 mag brightening.

Extensive computer simulations of the eclipse have been performed, for testing the possible geometrical configurations of the eclipsing body, which are capable of generating light curves close enough to those observed. The method and the results are described in the Sections 4 and 5 following; application to previous eclipses is shown in Sect. 6.

4. Light-curve modelling

The thin-disk structure of the eclipsing body will be studied here, by using the method of the synthetic light curve. For a given configuration of the eclipsing disk (size, spatial orientation, opacity distribution), a theoretical light curve can be determined, by computing the effective portion of stellar surface which remains visible, at fixed time intervals (e.g. 10 days). The computation is performed by inscribing the image of the stellar surface in a grid of $100 \cdot 100$ elements, and by determining the contribution to the total luminosity given by each pixel (depending on its position with respect to the eclipsing body, a single pixel may be visible, occulted or partially absorbed).

By a suitable choice of the configuration parameters, a synthetic light curve is obtained, reproducing as closely as possible the observational data at a given wavelength. Then, the possibility of alternative configurations of the disk is explored, reproducing the observational light curve as well (within the limits of experimental accuracy and of spurious variability effects). In fact, the purpose of this investigation is to identify *univocally* (when possible) the main structural features of the object that are responsible for the observed eclipse.

Some reasonable simplifications can be introduced at this point in order to reduce the number (potentially infinite) of possibilities to be examined. First of all, let us establish for each model parameter the accuracy to be considered. Numerical testings suggest that small but still appreciable effects on the light curve can be produced by changing the geometry of the disk (e.g. the hole radius) by about $1/100$ of the disk size, that is by steps of 0.1 AU. Similarly, in order to change the model light curve appreciably, the inclination of the disk can be varied by steps of 0.1° ; while the opacity of the semitransparent zones must change by about $1\% \div 10\%$ (depending on the extension of the zone).

Circular symmetry can be assumed, as a first approximation for the opacity distribution inside the disk. Moreover, no significant structure should be recognizable in the disk, at scales smaller than the size of the star (which behaves as a scanning beam through the eclipsing body). This allows us to describe the opacity distribution in the disk, by considering no more than 5 concentric bands (thus excluding the possibility of detecting thin ringlets)

Let us recall that the *thin-disk* model conventionally assumes the disk is planar, and that its thickness is small. In fact, some light of the star is able to reach the observer, after passing through the central hole at an incidence of $5^\circ \div 10^\circ$ (that is the disk inclination). This condition limits the possible thickness of the disk; in particular, the observed mid-eclipse brightening

is hardly compatible with a disk thickness (at the hole's edge) larger than $\sim 5\%$ of the disk size. Moreover, the shape of the light curve reveals the existence of a narrow annular gap in the disk, through which the stellar surface is also seen (Sect. 5.2); this provides a further constraint for the disk thickness, which should be less than $\sim 2\%$ of the disk size. Hence, in our geometrical approximation, we shall assume that the thickness of the disk is very small, e.g. $\sim 1\%$ of the disk size (that is about 0.1 AU) or less.

So, allowing for some obvious simplifications, the survey of the possible configurations of the eclipsing body has been carried out systematically; the simplest structures have been considered first, and only when necessary have more complex options been introduced. The geometrical parameters have been varied step by step, independently and also in a combined fashion, in order to establish, for each parameter, a best-fit value (if possible) or at least a complete set of acceptable values.

Unfortunately, because of intrinsic stellar variability superimposed on the light curve of the eclipse, any fitting procedure will be limited, since it will fail to reproduce these irregular features. However, some kind of discrimination is possible, since intrinsic variability is strongly wavelength-dependent, and increased towards the UV; a multi-wavelength analysis of the eclipse is then required.

5. The 1983 eclipse

5.1. General

To initialize the computation, approximate values have been introduced for eclipse timing: the orbital period $P = 9885$ d (Gyldenkerne, 1970); and the time t of mid eclipse, $JD = 2445500$. Final best-fit results (based also on previous eclipses) are the following: $P = 9890$ d; $JD = 2445505$. A probable uncertainty of ± 5 d (that is only 1% of the eclipse duration) is related to these values, because the occulting body may change a little its shape in different eclipses (Sect. 6), thus slightly altering the regularity of eclipse timing.

Assuming the primary's radius r as unit length, the orbital separation a can be derived from the duration of partial-eclipse phases, which is on average ~ 110 d (Schmidtke, 1985; with 10 d prolongation for compensating out-of-eclipse pulsations). The duration of a single partial phase shows how much time is taken by the eclipsing body to advance along its orbit by one stellar diameter. For a circular orbit, we have simply $2\pi a/2r = 9890/110$, so that the separation is $a = 28.6$ units ($r = 1$). A more accurate result will be obtained by including the eccentricity (Wright, 1970) in the calculations. Anyway, a non-equatorial transit, or a semitransparent edge of the eclipsing body, may shorten or lengthen the partial phases respectively, thus leading to a corresponding over- or under- estimation of the orbital size.

Considering these circumstances, a reasonable value for orbital separation can be simply $a = 28.6$ units. The estimated probable uncertainty is ± 3 units (allowing for possible 10-day misinterpreted distortion of partial phases). This leads to a corresponding 10% uncertainty in the relative proportions of the eclipsing body with respect to the primary star. Thanks to a lucky numerical coincidence, the orbital separation predicted by the large-mass scenario ($m_1 = 15.5 M_\odot$; $m_2 = 13.9 M_\odot$) is just $a \simeq 28$ AU (Takeuti, 1986). Hence, the *unit length* used in this analysis of the eclipse (primary's radius) can be practically

identified with the *Astronomical Unit* in the large-mass scenario. Hereafter, the large-mass model will be generally assumed as a convenient reference, so that all the lengths will be expressed directly in AU.

However, if the low-mass model is preferred ($m_1 = 1.33 M_\odot$; $m_2 = 5 M_\odot$), then the predicted separation is $a = 16.7$ AU. In this case, it will be necessary to scale down the size of the system proportionally, by multiplying all the lengths by the conversion factor of 0.6.

5.2. Equatorial eclipse: the ring-like structure

As an initial simplified approach, let us consider – at visible wavelength – an equatorial eclipse produced by a planar disk, which is inclined towards the observer (but not laterally tilted). That is the case when the inclination of the orbital plane (with respect to the plane of the sky) is $i = 90^\circ$, while the inclination of the disk plane (with respect to the plane of the sky) is $j < 90^\circ$, and the lateral tilt of the disk (angle between the projected-disk's major axis and the projected-orbit's major axis) is $\psi = 0^\circ$.

We want to stress that the planar-disk approach, used hereafter, is only a convenient simplification. In fact, it has been shown that the disk should be *warped*, having a twisted structure (Kumar, 1987). But for studying these more complex features, a refinement of the present method would be required.

The first striking result of numerical simulations of the eclipse is that a simple uniform disk with a central hole – in other words, a single ring – does *not* fit the observed light curve, since one finds that the well-known profile of totality (flat bottom plus central peak) can not be matched. More precisely, there is no way to reproduce the *flat bottom* of totality, because the light curve generated by a *single ring* has a smooth shape (vaguely resembling the letter W), with two *rounded minima* flanking a central hump (Fig. 1, dashed line).

Such a fact, which was first envisaged by Ferluga (1989) using numerical computations, is indeed a direct consequence of the assumed geometry of the eclipsing body (oblique flat ring). Let us now discuss this point in more detail.

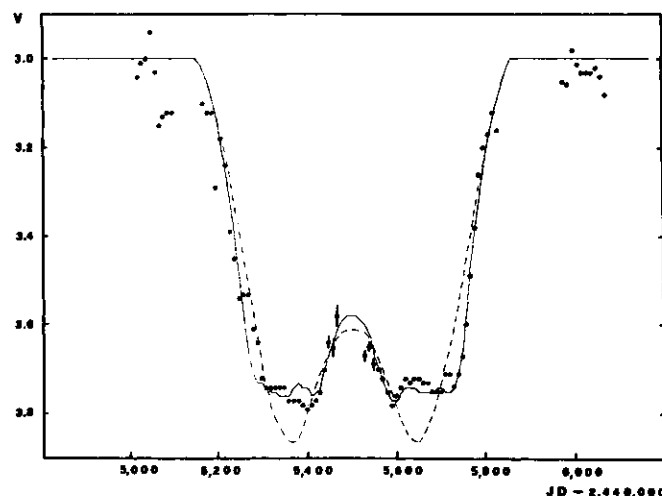


Fig. 1. Light curve of the 1983 eclipse. Dots: V data by Schmidtke (1985). Dashed line: single-ring model. Solid line: split ring, with transparent annular gap (equatorial eclipse).

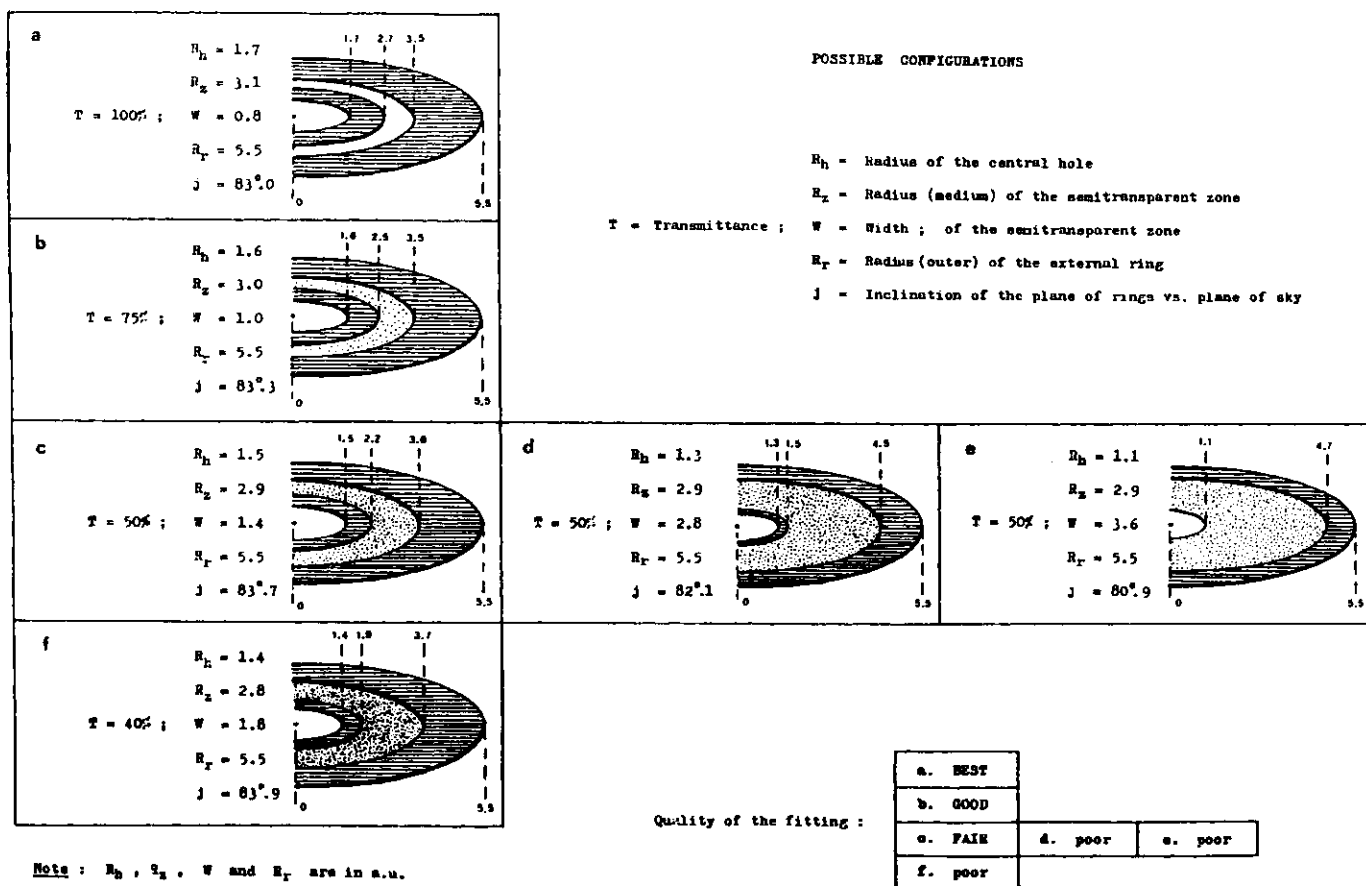


Fig. 2. Possible configurations, fitting the V light curve on 1983 (equatorial transit); for clarity's sake, the disk's inclination j has been exaggerated in the pictures. Cases *a*, *b*, *c* produce a better fit, and are summarized in Table 2; case *a* is that of Fig. 1 (solid line).

Being thin, circular and inclined, the occulting body will be seen in perspective as a dark ellipse with a very elongated aspect ratio (about 10:1), projected over the primacy's surface and over the background sky. During the eclipse, this elliptical object will transit along the stellar equator, by advancing sideways on the major axis (which is about 5 times the stellar diameter). Thus, it will appear as a dark *equatorial band* projected over the star; but the height of this band will vary during totality, as different portions of the dark ellipse transit in front of the star. In fact, the dark band will be thicker at mid totality (when the central portion of the ellipse is interposed), while it will be thinner during the initial and final part of totality (when the apsidal portions of the ellipse are interposed). Hence, during the first and last part of totality, the resulting light curve will display a gradual deepening towards mid eclipse, with a *smooth* bend (and not a rigid flattening) at the 2nd and 3rd contacts.

Because of inclination, also the inner hole will be seen as an elongated elliptical aperture (slightly longer than the stellar diameter), transiting in front of the star at about mid totality. The amount of stellar light passing through the hole is going to increase gradually until mid eclipse, when the aperture will be centrally aligned (with its widest part in front of the star). Such additional luminosity will invert the deepening trend of the light curve towards mid totality, and it will cause the rising of the mid-eclipse bump. The rising of this peak from the bottom of totality is expected to be gradual, almost as *smooth* as the 2nd and 3rd contacts (for similar reasons).

Moreover, because of the length and size of the mid-eclipse brightening, its smooth "roots" should be practically connected with the smooth bends at the 2nd and 3rd contacts; so that no space would remain for a flat totality "plateau"; and a light curve with two *rounded minima* would be produced. In fact, this is just the shape of the synthetic light curve, computed for the single-ring model (Fig. 1, dashed line). But the fitting with the experimental points (Fig. 1, dots) is not yet satisfactory.

Hence, one is forced to consider more complex structures, consisting of several rings with different transparencies. The simplest possibility is to introduce a *Cassini-like* gap, splitting the main opaque ring into 2 concentric parts. This would provide the additional light required to render the bottom of totality flat on both sides of the central peak.

In general, the flat bottom of totality can be produced by an annular *semitransparent band* of suitable extension (Fig. 2). This involves four discontinuities in the radial distribution of opacity: r_1 (hole's radius), r_2 (band's inner edge), r_3 (band's outer edge), r_4 (disk's radius). Configurations *a*, *b*, *c*, and intermediate ones, reproduce the observed light curve very well (Fig. 1, solid line), as far as this is allowed by superimposed pulsations of the F supergiant; this family of possible solutions is summarized in Table 1.

Alternative configurations, with a wider 50%-transmittant zone (*d*, *e*), or with lower transparencies (*f*), are not favoured since they produce a mid-eclipse brightening which is not sharp enough. Finally, let us stress in Fig. 2 the large

Table 1. Equatorial eclipse.

gap's transmittance	$T = (75 \pm 25) \%$
disk's obliquity	$j = 83^\circ.3 [-.3 \setminus +.4]$
hole radius (r_1)	$R(h) = 1.6 \pm .1 \text{ AU}$
gap's radius ($(r_1+r_2)/2$)	$R(z) = 3.0 \pm .1 \text{ AU}$
gap's width (r_2-r_1)	$W = 1.0 [-.2 \setminus +.4] \text{ AU}$
disk radius (r_4)	$R = 5.5 \text{ AU}$

"horizontal" family of configurations (*c*, *d*, *e* and intermediate ones) with an extended 50% transmittant zone: these solutions (although poorly fitting the brightening) reproduce the general 50% absorption corresponding to the eclipse depth of ~ 0.75 mag.

5.3. Tilted disk

Photopolarimetric observations of the eclipse (Kemp *et al.*, 1986) provide significant indications about the orbital inclination *i* and about the disk's tilt ψ . This determination is particularly reliable, because the orbital orientation found by polarimetry is in excellent agreement with the astrometric orbit of the primary (Van de Kamp, 1978).

Let us then assume, in all the following discussion, the value of inclination $i = 89^\circ.4$ (implying a non-equatorial transit with a shift $H = 0.3$ stellar radii), and the value of the lateral tilt $\psi = 2^\circ.3$, both determined by photopolarimetry. This means we are going to consider a non-equatorial eclipse, produced by an obliquely tilted disk (Table 2).

For the above conditions, the family of solutions which fits better the light curve, still corresponds qualitatively to the configurations *a*, *b*, *c* and intermediate ones (Fig. 2); but some minor adjustments are required. In particular, with respect to the values on Table 1, the disk's obliquity *j* should be decreased by 1° (less grazing incidence), and the radius *R* should be reduced by 0.1 AU (slightly smaller disk).

There is moreover one problem, which has been envisaged by Kemp *et al.* (1986), when they suggested the configuration with $i = 89^\circ.4$, $\psi = 2^\circ.3$ (although the mid-eclipse brightening was not considered). This configuration should produce an *asymmetric* eclipse, much more distorted than the observed one. In particular, numerical simulations show that the bottom of totality should slope downward, towards the 3rd contact, by about 20% of the

Table 2. System parameters.

orbital period	$P = 9890 \pm 5 \text{ d}$
JD of mid-eclipse (1983)	$t = 2,445,505 \pm 5$
primary's radius	$r = 1.0 \pm .1 \text{ AU}$
orbital separation	$a = 28.6 \pm 3 \text{ AU}$
orbital inclination	$i = 89^\circ.4 \pm .3$
disk's inclination	$j = 82^\circ.0 \pm 1^\circ$
disk's lateral tilt	$\psi = 2^\circ.3 \mp 1^\circ$

eclipse depth. But this does not happen: for example, the *V* light curve seems compatible only with less than 1/2 of the shift and tilt indicated by polarimetry.

On the other side, the expected asymmetry is gradually revealed at shorter wavelengths in the UV (Ake, 1985). Different explanations for this effect may be considered: selective limb-darkening, reddening in the disk, or asymmetry of the disk itself. Numerical simulations suggest an asymmetry of the semitransparent Cassini-like band, which should be $\sim 25\%$ narrower on the forward side of the disk (in the sense of orbital motion), and correspondingly wider on the back side. This asymmetric band would provide the right contribution of light, required for balancing the slope of totality at visible wavelengths. Being semitransparent, this zone may produce *reddening* in the most natural way, $E(B - V) = A(V)/3$; so at shorter wavelengths it would be more opaque, and thus less effective in masking the downslope of totality. Simulations indicate that the transmittance in the *V* band should be very high: $\sim 90\%$ or more.

Although in this case it might be considered an ad hoc assumption, radial asymmetry in the eclipsing body is probably necessary, since during the 1956 eclipse an asymmetric negative bump was observed on totality (Fig. 7, dots). In our simplified model, radial asymmetries are treated as follows. The centers of circles defining the opacity bands (radii r_1, r_2, r_3, r_4) may be displaced along the direction of orbital motion by corresponding *offsets* x_1, x_2, x_3, x_4 . Note that this is only a convenient approximation, accounting for the resolution limits of our method; in principle also a spiral structure, seen at grazing Aincidence, could resemble a system of off-center rings!

5.4. Multi-wavelength analysis

As we have seen, a multi-band fitting procedure is required for a complete understanding of the structure of the eclipsing body. But a fine analysis will also consider, besides totality, the behaviour of partial phases; for example, the slopes of ingress and egress are considerably different.

First of all, it is necessary to clear the light-curve data from the superimposed intrinsic variations; these are often called *F-star's pulsations*, although variability may come, as well, from the hot source in the eclipsing body, as suggested by UV observations of the eclipse (Boehm, Ferluga and Hack, 1984). Anyway, this variability increases substantially toward the shorter wavelengths. Hence, it is sufficient to consider the difference between two (normalized) UV light curves at 1900 Å and 2850 Å, to have the necessary record of intrinsic fluctuations. These appear in the UV as irregular peaks of about 50 days' duration (pseudoperiod ~ 100 d).

At visible wavelengths, one can scale-down the intrinsic UV fluctuations by a suitable factor (35%, 15%, 10% for *U*, *B*, *V* respectively), and subtract them from the observed light curve; thus providing some restoration of the true profile of the eclipse phases. By this procedure, light-curve fluctuations are reduced, (although not completely removed, since probably not all the peaks have the same radiation temperature). This is a significant result (Figures 3, 4, 5; asterisks), because it allows the identification of those light-curve features, which are *not* eclipse-dependent (e.g. the "shoulder" before the 2nd contact, and the small bumps near the 3rd and 4th contacts). As expected, the mid-eclipse brightening remains substantially unchanged.

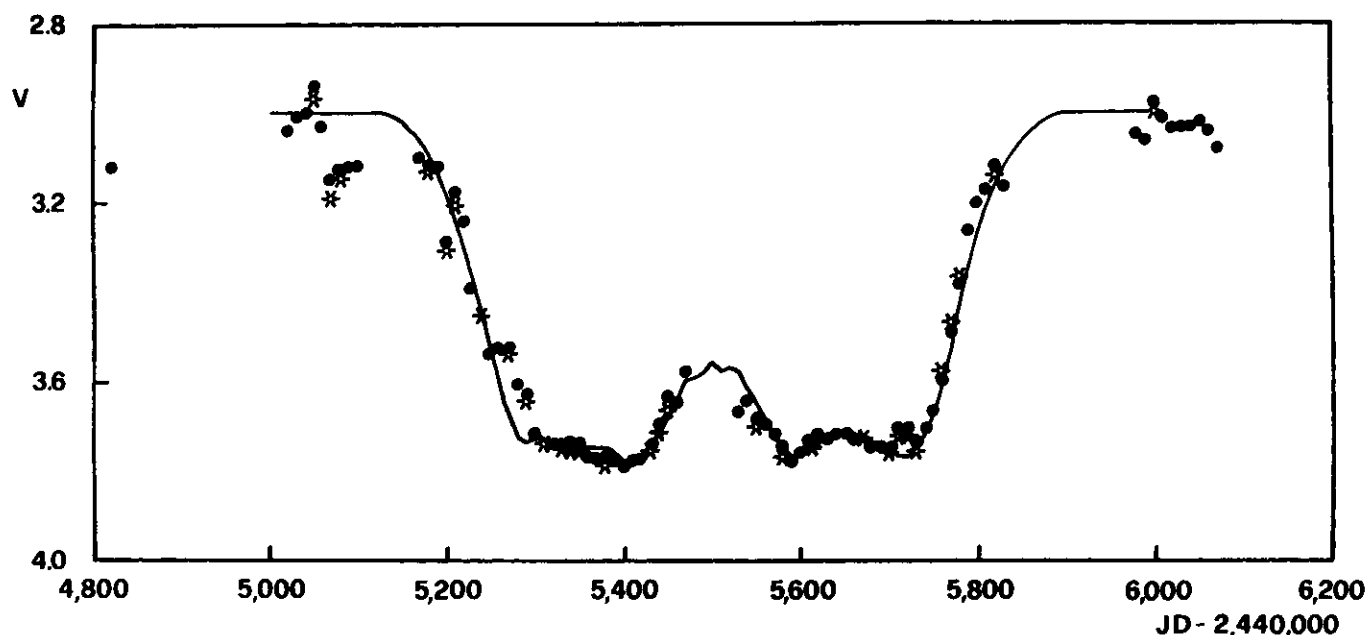


Fig. 3. 1983 eclipses: V data (dots), compared with the synthetic light curve (solid line) of the tilted-disk model (Tables 2, 3). The quality of the fitting is excellent.

After this refinement, the profile of partial phases proves to be more symmetrical and, in particular, smoother than would be expected from the kind of eclipsing disk considered up to now (which has a sharp outer edge at 5.4 AU). As has been said, this effect could also depend on an error in the estimation of the orbital separation. But, since the preceding eclipses show partial phases of still different (much smoother) shapes, this is evidence that the eclipsing disk has a semitransparent edge, varying in size from one eclipse to another.

Thus, to fit the V light curve, we have considered a 50%-transmittant outer ring of suitable width (0.9 AU), replacing the sharp edge at 5.4 AU. Obviously, this is only a schematic representation of the disk's edge, which probably vanishes gradually going outwards. Standard reddening from this external zone accounts, by itself, for the colour-dependent asymmetry of the light curves throughout the eclipse, in a still better way than could be done by a highly-transparent ($\sim 90\%$) "Cassini" gap (which would be effective only on totality). So, in conclusion, we may consider the Cassini-like zone to be almost 100%-transparent, giving only a minor contribution to the reddening effects of the eclipse.

5.5. Results

With the identification of the outer semitransparent ring (external radius r_5), the total number of distinct annular zones considered in the disk has reached the limit of resolution discussed above (Sec. 4). Any further attempt, of identifying finer details in the disk, will not be very significant (leading to non-univocal determinations).

As the foregoing discussion has shown, the best multi-wavelength fitting is obtained for a Cassini-like zone which is $\sim 100\%$ transparent. This implies corresponding well-defined values for the other parameters (upper-script values on Table 1). The resulting final configuration of the system is given in Tables 2

Table 3. The 1983 disk. - (*) Note: T_i is the transmittance (%) within r_i ; T_5 is for $V, B, U, UV(2850 \text{ \AA})$.

rings (AU)	transmittances (*)	offsets (AU)
$r_i \pm .1$	$T_i \pm 10$	$x_i \pm .1$
$r_1 = 1.6$	$T_1 = 100$	$x_1 = 0$
$r_2 = 2.7$	$T_2 = 0$	$x_2 = +.1$
$r_3 = 3.5$	$T_3 = 100$	$x_3 = -.1$
$r_4 = 5.0$	$T_4 = 0$	$x_4 = +.1$
$r_5 = 5.9$	$T_5 = 50, 40, 30, 10$	$x_5 = 0$

and 3, accounting also for the constraints by polarimetry and for the smooth-edge implementation. The quality of the fitting can be appreciated in Figures 3, 4, 5, and 6, referring to V, B, U , and $UV(2850 \text{ \AA})$, respectively.

Probable uncertainties in Tables 2 and 3 are intended only as qualitative indications about the sensitivity of the method, and about the different degrees of reliability of the parameters. The errors of 0.1 AU in r_i and in x_i are only those depending on the fitting accuracy; uncertainties Δr_i are mutually correlated quantities, and could eventually be larger because of poorly-compensated intrinsic variability. The angles i and ψ have been assigned an uncertainty corresponding to 1/2 of the polarimetric values of shift and tilt.

Finally, the fundamental possibility of size-scaling factors should be kept in mind. Values in AU of the primary's radius r , of the separation a , and of the rings' radii r_i , are referred to the large-mass model ($q \approx 1$); thus they should be multiplied by 0.6, when the low-mass model ($q \approx 1/4$) is considered.

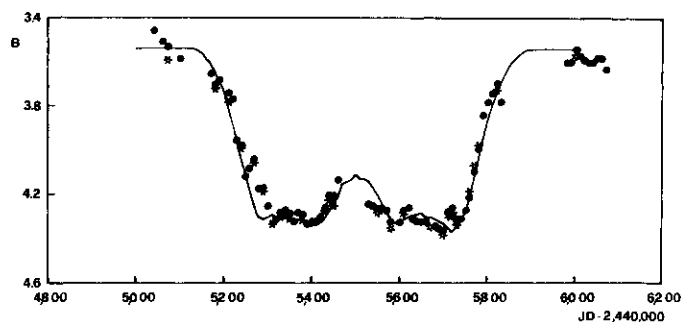


Fig. 4. 1983 eclipse : B data (dots) ; same model as in Fig. 3. The fitting gets worse toward shorter wavelengths, because of overposed intrinsic variability.

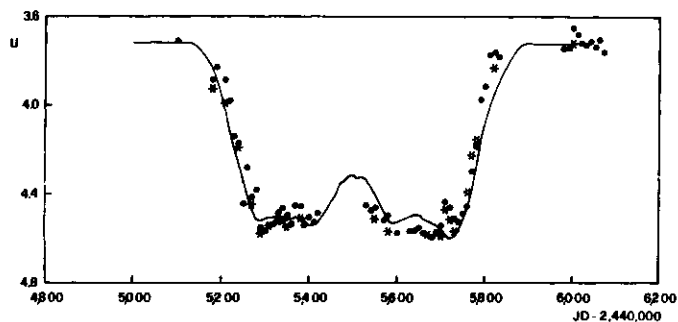


Fig. 5. 1983 eclipse : U data (dots) ; same model. Note that the values corrected for intrinsic variability (asterisks) are closer to the synthetic light curve (solid line).

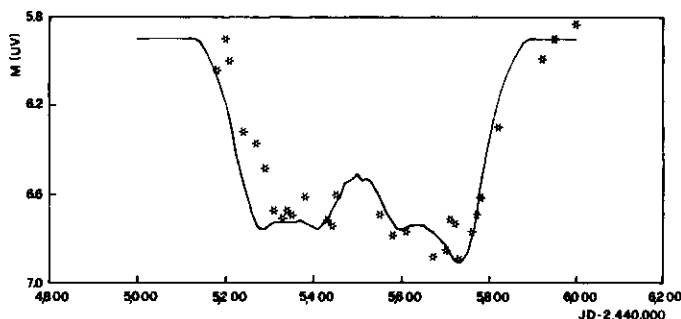


Fig. 6. 1983 eclipse : UV ; $\lambda = 2850 \text{ \AA}$ (Ake, 1985). Note the fitting of totality's downslope, from 2nd to 3rd contact. The curve in the UV is very much disturbed by intrinsic variability.

6. The preceding eclipses

The light curve of ϵ Aur repeats itself in the different eclipses, with some irregular modifications: in particular, the depth and duration of totality, and the presence of (almost-grey) positive or negative bumps. Considering the last three eclipses (which are the only well-documented ones), there is *no* systematic trend in these secondary alterations; hence they can not be ascribed to precession effects. The only possible explanation is, then, in terms of structural variations of the eclipsing body. We now, however, that precession *should* occur for a tilted disk; as an effect one should observe a slow modification of the angles j and ψ , but its detection seems beyond the capability of the present analysis.

Table 4. The 1956 disk.

rings (AU)	transmittances (%)	offsets (AU)
$r_i \pm .1$	$T_i \pm 10$	$x_i \pm .1$
$r_1 = 1.3$	$T_1 = 100$	$x_1 = -.7$
$r_2 = 2.3$	$T_2 = 0$	$x_2 = -.5$
$r_3 = 2.9$	$T_3 = 100$	$x_3 = -.3$
$r_4 = 4.4$	$T_4 = 0$	$x_4 = +.1$
$r_5 = 5.7$	$T_5 = 50$	$x_5 = -.1$

Table 5. The 1929 disk.

rings (AU)	transmittances (%)	offsets (AU)
$r_i \pm .1$	$T_i \pm 10$	$x_i \pm .1$
$r_1 = 0.9$	$T_1 = 100$	$x_1 = 0$
$r_2 = 2.0$	$T_2 = 0$	$x_2 = 0$
$r_3 = 2.7$	$T_3 = 100$	$x_3 = -.1$
$r_4 = 4.3$	$T_4 = 0$	$x_4 = +.1$
$r_5 = 5.9$	$T_5 = 50$	$x_5 = -.1$

In order to ensure a homogeneous comparison of the 3 eclipses, when analysing the preceding two events of 1956 and 1929 one must adopt the same method as for the last eclipse. The large-mass scenario is still considered, and the orbital terms remain those of Table 2; the only parameters which will be allowed to change are those defining the configuration of the rings: radii r_i , transmittances T_i , and offsets x_i (with $i = 1, \dots, 5$).

For the *1956 eclipse*, the fitting (V band) is shown on Fig. 7 (solid line), compared with the thick-disk model (dashed line) by Huang (1974); the resulting configuration is given on Table 4

(where the accuracy is the same as in Table 3). In this eclipse, with respect to the most recent one, the outer semitransparent band is much wider (1.3 AU), while the inner configuration of the disk is reduced in size by about 10%. Note the asymmetry of the inner rings (the hole is shifted backwards by 0.7 AU), which is required for fitting the displaced negative bump. Moreover, the fact that the bump is still sharper than the one reproduced by the model, suggests the presence of a broken ring, or of a single thick cloud (eventually extending off-plane).

For the older *1929 eclipse*, the fitting (P band) is displayed on Fig. 8, compared with the single-ring model (dashed line) by Wilson (1971); the resulting configuration is reported on Table 5.

In this case the outer semitransparent band is even larger (1.6 AU), accounting for the smooth slope of partial phases. Since totality is almost flat, there are no constraints helping to determine the inner parts of the disk unambiguously. So the values of r_1 , r_2 , r_3 (and related T_i ; x_i) are not fixed, unless one assumes a priori that the main features of the disk are kept the same, as in the other eclipses (central hole and "Cassini" gap, both transparent). In principle, an extended semitransparent

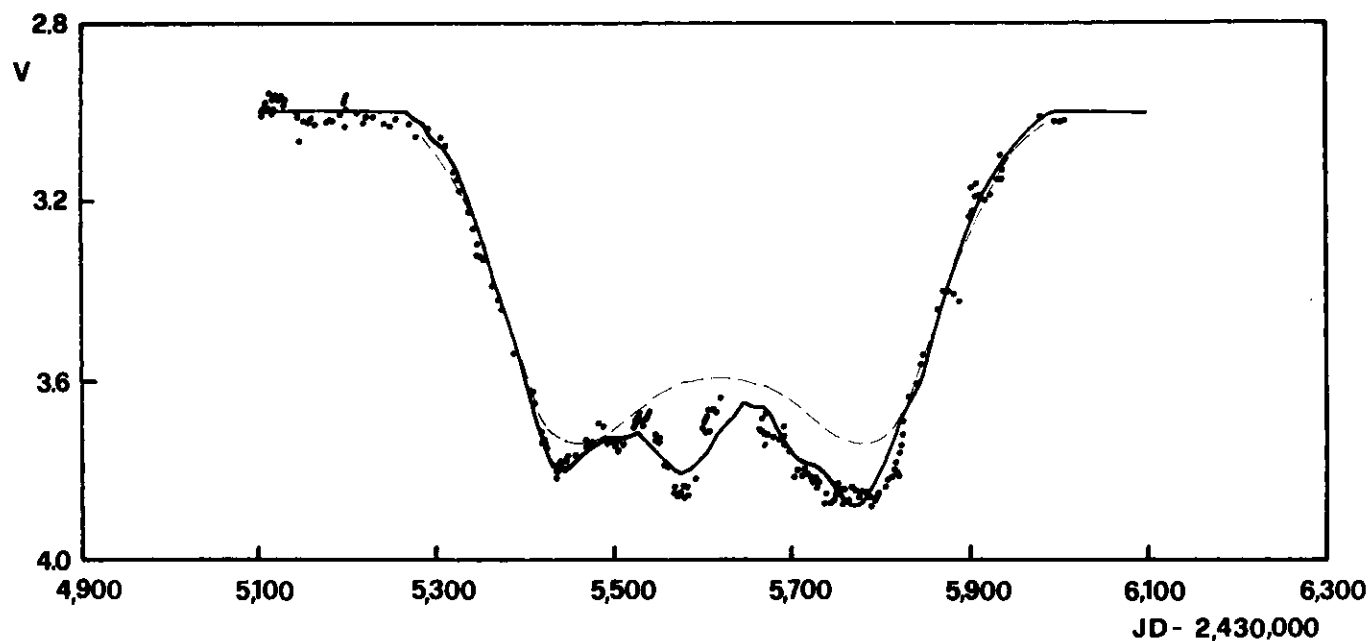


Fig. 7. 1956 eclipse : V data (dots). The synthetic curve (solid line) is compared with the old model (dashed line) by Huang (1974).

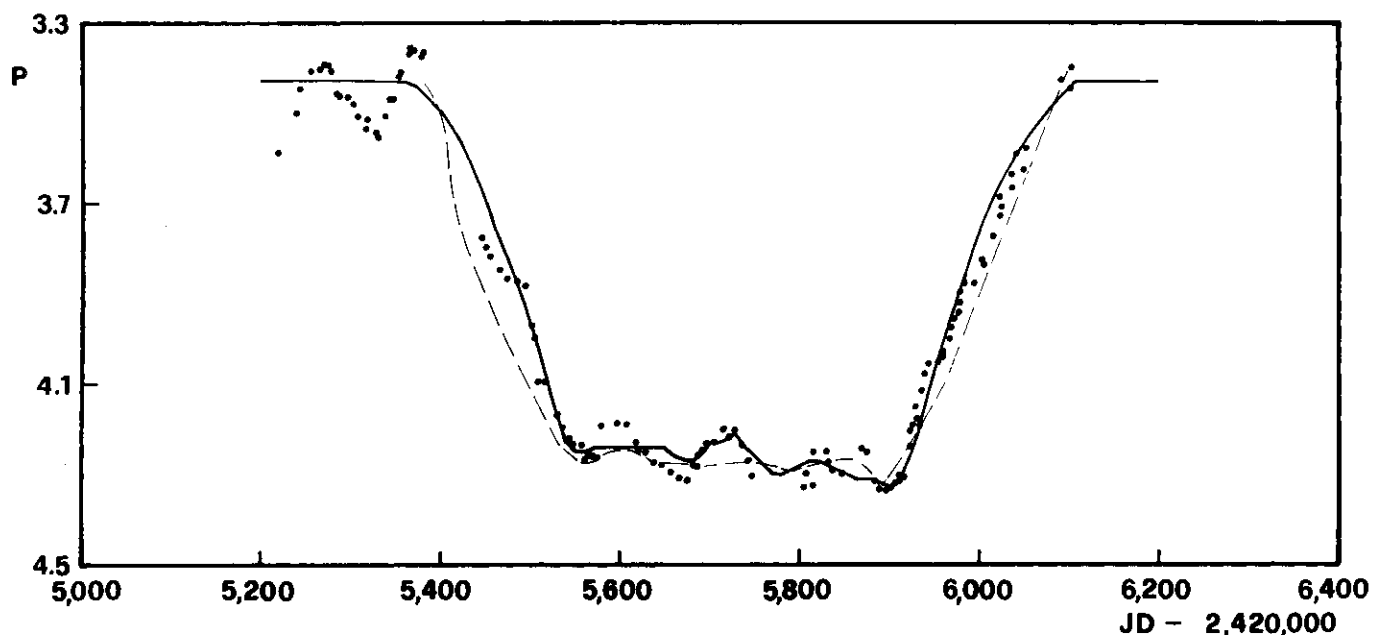


Fig. 8. 1929 eclipse : P data (dots). The synthetic curve (solid line) is compared with the old model (dashed line) by Wilson (1971).

inner zone like that in Fig. 2e (with smaller hole), may account as well for the observed light curve. A final element of uncertainty is given by the strong intrinsic variability (and/or experimental errors), reaching ± 0.1 mag out of eclipse, and thus masking the finer details of the occultation.

7. Discussion and conclusions

A physical analysis of the disk structure is beyond the purpose of the present work. But some basic aspects can be pointed out.

The dynamical stability of single-particle orbits in the system of ϵ Aur has been analysed by Van Hamme and Wilson (1986), considering the triple-system model, where the secondary is supposed to be a close binary embedded at the center of the disk. It was found that the stable orbits around the secondary define a thin disk with a central hole; the disk's external radius r_{outer} and the internal radius r_{inner} depend on the separation of the close binary which also perturbs the inner disk with its strong UV activity and with angular-momentum transfer). To be compatible with the size of the hole in different eclipses ($r_1 = 1.3 \pm .4$ AU), this separation must be ~ 0.6 AU or smaller. This implies the following possibilities for the disk's radius: $r_{\text{outer}} = 5.2$ AU,

or $r_{\text{outer}} = 4.4 \text{ AU}$, for the *high-mass* and *low-mass* models respectively.

Let us compare these theoretical predictions with our determination of the smooth outer edge of the disk, that is the semitransparent external band. Its extension in the high-mass scenario (Tables 3, 4, 5), is between $r_4 = 4.6 \pm .4 \text{ AU}$ and $r_5 = 5.8 \pm .1 \text{ AU}$ (considering all the three eclipses). The radius at mid band $(r_4 + r_5)/2$, which corresponds to the disk's radius R in the sharp-edge approximation, is then precisely $R = 5.2 \pm .2 \text{ AU}$. This value coincides with the theoretical disk radius $r_{\text{outer}} = 5.2 \text{ AU}$, predicted for the same high-mass scenario!

On the contrary, if the low-mass model is assumed, all proportions of the observed disk should be scaled-down by the factor 0.6. This would lead to the following radii: $r_4 \simeq 2.8 \text{ AU}$, $r_5 \simeq 3.5 \text{ AU}$, and $R = 3.1 \text{ AU}$. In this case, there would be *no* correlation with the theoretical value $r_{\text{outer}} = 4.4 \text{ AU}$, predicted for this low-mass model. However, in principle, one cannot exclude the possibility that the disk may have a small size, not depending on this kind of stability constraints.

In conclusion, the close agreement between the observed radius and the dynamical limit, for the (triple-system) large-mass model, provides support in favour of this conception of *ϵ Aur*. The existence of a variable semitransparent annular band around the limit of stable orbits suggests the settling of material onto the disk. This band shows an asymmetry, which consists of a "stretching", in the direction opposite to the motion (of the eclipsing body along its orbit): the band's width is $\sim 1.4 \text{ AU}$ on the backward part of the disk, and only $\sim 1.0 \text{ AU}$ on the forward part. Moreover, also the Cassini-like semitransparent gap behaves in a similar way.

This is just expected, if some diffuse material coming from the primary's stellar wind is conveyed into the secondary Roche lobe, joining the rear border of the rotating disk, and there condensing into a stable external ring of dust. The observed enhancement of the *shell lines* on egress (Ferluga and Hack, 1985), indicates a denser gaseous envelope on the rear side of the eclipsing body, and the detection of molecular CO lines only on egress (Hinkle and Simon, 1987), does in fact confirm such a concept.

A fine analysis of the shell spectrum (work in progress) shows that the structure of the gaseous envelope is approximately toroidal, surrounding the semitransparent edge of the disk, with a remarkable off-plane extension ($\simeq 1 \text{ AU}$). Besides revealing a significant gas-dust-ring connection, this "atmosphere" (thicker at 3rd contact) may also explain the over-estimation of the disk tilt (deepening of 3rd contact) derived by polarimetry.

Finally, let us complete the picture by suggesting a possible mechanism for the internal ring structure. The high temperature of the inner parts of the eclipsing body (Boehm and Ferluga, 1986) due to the central variable hot source (Boehm, Ferluga and Hack, 1984), and the angular-momentum perturbations by

the inner binary, will cause the dust to vaporize and to be "blown-off" from the central region, thus possibly forming an irregular ring-like cloud (occasionally extending off-plane), near the inner stability limit.

In this scenario, the physical mechanism producing the Cassini-like gap has still to be clarified (the similarity with Saturn is obviously accidental). Important information, about the physical conditions inside the gap and the central hole, should be obtained by studying in detail the shell spectrum during totality.

Acknowledgements. The author is grateful to M. Hack for stimulating discussions, and to S. Kumar for valuable comments. The computations were performed at the Astronet pole of Trieste.

References

- Ake, T. B.: 1985, in *The 1982–84 Eclipse of Epsilon Aurigae*, p. 27 (NASA Conf. Publ. no. 2384; Stencel, ed.)
- Boehm, C., Ferluga, S., Hack, M.: 1984, *Astron. Astrophys.* **130**, 419
- Boehm, C., Ferluga, S.: 1986, *Highlights of Astronomy* **7**, 201
- Eggleton, P. P., Pringle, J. E.: 1985, *Astrophys. J.* **288**, 275.
- Ferluga, S., Hack, M.: 1985, *Astron. Astrophys.* **144**, 395
- Ferluga, S.: 1989, *Memorie Soc. Astron. Italiana* **60**, 211
- Gyldenkerne, K.: 1970, *Vistas in Astron.* **12**, 199
- Hinkle, H. K., Simon, T.: 1987, *Astrophys. J.* **315**, 296
- Huang, S.-S.: 1974, *Astrophys. J.* **189**, 495
- Kemp, J. C., Henson, G. D., Kraus, D. J., Beardsley, I. S., Carrol, L., Ake, T. B., Simon, T., Collins, G. V.: 1986, *Astrophys. J.* **300**, L11
- Kumar, S.: 1987, *Monthly Notices Royal Astron. Soc.* **225**, 823
- Lissauer, J. J., Backman, D. E.: 1984, *Astrophys. J.* **286**, L39
- Ôki, T., Sekiya, I., Hiramaya, K.: 1984, *IAU Inform. Bull. Variable Stars* no. 2509.
- Schmidtke, P. C.: 1985, in *The 1982–84 Eclipse of Epsilon Aurigae*, p. 67 (NASA Conf. Publ. no. 2384; Stencel, ed.)
- Stencel, R. E. (editor): 1985, *The 1982–84 Eclipse of Epsilon Aurigae*, NASA Conference Publication no. 2384 (Tucson meeting)
- Swings, J.-P. (editor): 1986, *Highlights of Astronomy* **7**, 143–206 (Joint Disc. on Long-P Eclipsing Binaries; XIX IAU Assemb.)
- Takeuti, M.: 1986, *Astrophys. Space Sci.* **120**, 1
- Van De Kamp, P.: 1978, *Astron. J.* **83**, 975
- Van Hamme, V., Wilson, R. E.: 1986, *Astrophys. J.* **306**, L33
- Wilson, R. E.: 1971, *Astrophys. J.* **170**, 529
- Wright, K. O.: 1970, *Vistas in Astronomy* **12**, 150.

This article was processed by the author using Springer-Verlag T_EX AA macro package 1989.